2-1-1983

Excitation Spectrum and T = 0 Dynamics of the One-Dimensinal Anisotropic Antiferromagnet

Mahalingam Mohan

Gerhard Müller
University of Rhode Island, gmuller@uri.edu

Citation/Publisher Attribution

Mahalingam Mohan and Gerhard Müller. *Excitation spectrum and T=0 dynamics of the one-dimensinal anisotropic antiferromagnet.* Phys. Rev. B **27** (1983), 1776-1783.
Available at: http://dx.doi.org/10.1103/PhysRevB.27.1776

PHYSICAL REVIEW B VOLUME 27, NUMBER 3 1 FEBRUARY 1983

Excitation spectrum and $T=0$ dynamics of the one-dimensional anisotropic antiferromagnet

Mahalingam Mohan and Gerhard Müller*
Department of Physics, University of Rhode Island, Kingston, Rhode Island 02881
(Received 19 August 1982)

Recent low-temperature inelastic neutron scattering data on the quasi-one-dimensional (1D) Heisenberg-Ising antiferromagnet (AFM) $CsCoCl_3$ call for new theoretical efforts, for the available theories fail to explain the observed line shapes. In this paper we initiate a detailed study of the dynamical properties of the 1D spin-$\frac{1}{2}$ anisotropic XYZ AFM with emphasis on the dynamic structure factor $S_{\mu\mu}(q,\omega)$ at $T=0$. The structure of $S_{\mu\mu}(q,\omega)$ is determined by the combined effects of the density of states and the matrix elements. Both effects are discussed for selected cases: the XY-Heisenberg AFM (planar system), the Heisenberg-Ising AFM (uniaxial system), and the XY-Ising AFM (biaxial system). The exact solution for $S_{zz}(q,\omega)$ of the XY-Ising AFM has already many features in common with the experimental data on $CsCoCl_3$. It is an ideal starting point for a perturbation approach to the Heisenberg-Ising AFM.

I. INTRODUCTION

One-dimensional (1D) classical and quantum spin Hamiltonians have been the subject of theoretical studies for quite some time.[1] The increasing interest in the time-dependent properties of integrable and "nearly integrable" Hamiltonians has resulted in the development and use of approximate schemes for their investigation. These approaches draw upon a combination of existing exact results and the now widely popular concepts of domain walls or solitons. Experiments measuring dynamical properties of quasi-1D magnets are analyzed in the light of these approaches with partial success. Some basic discrepancies between theory and experiment have remained. Available theories, for example, have failed to explain the observed line shapes of recent low-temperature inelastic neutron scattering experiments on the quasi-1D Heisenberg-Ising antiferromagnetic (AFM) $CsCoCl_3$. Moreover, there is a general tendency to explain such discrepancies as being due to the inadequacy of simple model Hamiltonians rather than due to the drastic approximations involved in the solution of these models.

This situation provides a strong motivation to do exact calculations for simple models of experimental relevance, or to provide as sound a basis as possible from which to carry out approximate approaches. In this paper we direct our attention to the general 1D spin-$\frac{1}{2}$ XYZ AFM. It is described by the Hamiltonian

$$H(\gamma,\Delta)=J\sum_{l=1}^{N}[(1+\gamma)S_l^xS_{l+1}^x+(1-\gamma)S_l^yS_{l+1}^y+\Delta S_l^zS_{l+1}^z]\,. \quad (1.1)$$

All cases with purely AFM interaction can be represented by parameters confined to the triangle $0\leq\gamma\leq 1$, $0\leq\Delta\leq 1-\gamma$ in parameter space, as illustrated in Fig. 1. In studying the static and dynamic properties of this Hamiltonian we must take due account of the important role played by fluctuations. They prevent long-range order at all nonzero temperatures. Even at $T=0$, the ground-state configuration is in general very complicated due to quantum fluctuations. They cause large deviations from the predictions of linear spin-wave theory for both the excitation spectrum and the dynamic structure factors. The following models represented by the three sides of the triangle in Fig. 1 are of particular interest.

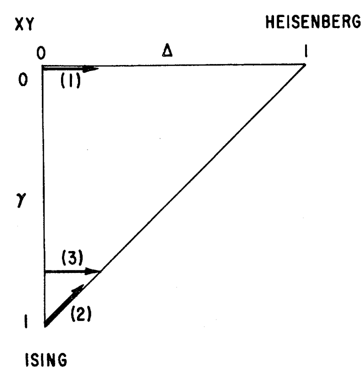

FIG. 1. Parameter space (γ,Δ) of the XYZ Hamiltonian $H(\gamma,\Delta)$. Triangle $0\leq\gamma\leq 1$, $0\leq\Delta\leq 1-\gamma$ represents the purely antiferromagnetic cases. Corners correspond to the familiar Heisenberg AFM $H(0,1)$, XY AFM $H(0,0)$, and Ising AFM $H(1,0)$. Arrows refer to perturbation approaches as explained in the text.

(i) The XY-Heisenberg AFM ($\gamma=0$, $0\leq\Delta\leq 1$). The $T=0$ dynamics of the planar AFM has been the subject of a recent comprehensive study. Analytic expressions for the $T=0$ dynamic structure factors $S_{zz}(q,\omega)$ and $S_{xx}(q,\omega)$ as defined in Eq. (2.7) below, have been conjectured on the basis of sum rules.[2–4] Furthermore, a perturbation calculation in the fermion representation has been performed,[5] starting at the exactly solvable $H(0,0)$ and using $H(0,\Delta)-H(0,0)$ as perturbation [see arrow marked (1) in Fig. 1]. $S_{zz}(q,\omega)$ has been evaluated for $\Delta \ll 1$ and $T=0$, yielding a result in agreement with the nonperturbative approach concerning both the excitation spectrum and the line shapes.[4,5] The results for $\Delta=1$ have been compared successfully with the data of inelastic neutron scattering experiments on the quasi-1D $S=\frac{1}{2}$ Heisenberg AFM $CuCl_2\cdot 2N(C_5D_5)$ (CPC).[6–8]

(ii) The Heisenberg-Ising AFM ($0\leq\gamma\leq 1$, $\Delta=1-\gamma$). The $T=0$ dynamics of the uniaxial AFM has been investigated by Ishimura and Shiba.[9] The trivially solvable Ising AFM $H(1,0)$ is the starting basis of their perturbation calculation, and $H(1-\Delta,\Delta)-H(1,0)$ is taken into account as a perturbation [see arrow marked (2) in Fig. 1]. To $O(\Delta)$ the calculation yields an excitation spectrum which is in reasonable agreement with exact results.[10] It predicts broad, slightly asymmetric peaks for both $S_{xx}(q,\omega)$ and $S_{zz}(q,\omega)$ at $T=0$ and fixed q as functions of ω (see Fig. 3 of Ref. 9).

$CsCoCl_3$ is a good physical realization of a highly anisotropic quasi-1D Heisenberg-Ising AFM ($\gamma=0.754$, $\Delta=1-\gamma$). Low-T inelastic neutron scattering experiments have recently been performed on $CsCoCl_3$ by Yoshizawa *et al.*[11] at Brookhaven National Laboratory and by Nagler *et al.*[12] at Chalk River Nuclear Laboratories. The experimental data of both groups reveal that the line shapes of $S_{zz}(q,\omega)$ are a great deal more asymmetric and more strongly peaked near the lower end of the continuum spectrum than predicted by the theory of Ref. 9 (see Fig. 9 of Ref. 11 and Fig. 3 of Ref. 12).[13] This discrepancy calls for further theoretical investigations.

(iii) The XY-Ising AFM ($0\leq\gamma\leq 1$, $\Delta=0$). The dynamics of the anisotropic XY model is amenable to rigorous calculations.[14–18] In Sec. III we present the exact expression for $S_{zz}(q,\omega)$ at $T=0$ in closed form. Although no physical realizations for this model are known as yet, $H(\gamma,0)$ is a good starting basis for a perturbation approach to the calculation of $S_{zz}(q,\omega)$ of the Heisenberg-Ising AFM.[19] In this approach, $H(\gamma,0)$ is represented by an exactly solvable system of noninteracting fermions and $H(\gamma,1-\gamma)-H(\gamma,0)$ is a fermion interaction [see arrow marked (3) in Fig. 1].

In this paper we initiate an investigation of the $T=0$ dynamics of the 1D $S=\frac{1}{2}$ XYZ AFM. The aim is to provide reliable results for the detailed structure of $S_{\mu\mu}(q,\omega)$ and, thereby, contribute to a better interpretation of the neutron scattering data on $CsCoCl_3$. In Sec. II, we discuss the exact excitation spectrum of the $S=\frac{1}{2}$ XYZ AFM and the corresponding density of states. The relevance of these excitations for the $T=0$ dynamics is investigated in Sec. III.

II. EXCITATION SPECTRUM OF THE XYZ AFM

Rigorous work on the 1D $S=\frac{1}{2}$ XYZ model was initiated in 1931 by Bethe.[20] He introduced a formalism for a representation of the eigenstates of the Heisenberg AFM as linear combinations of Ising-model eigenstates. This formalism was used later to calculate the energies of low-lying excited states of the XY-Heisenberg model and the Heisenberg-Ising model.[10,21–24] With the same technique, results were obtained also for the excitation spectrum of the XY-Heisenberg AFM in a magnetic field.[2,25] The excitation spectrum of the XY-Ising AFM has been derived in calculations using the fermion representation.[14–18,26,27] Rigorous results for the general Hamiltonian (1.1) became available only after the discovery of the mapping between the XYZ model and the exactly solvable eight-vertex model.[28,29] Johnson *et al.*[30] used this mapping for the determination of the energies of low-lying excited states for the XYZ model. They found as low-lying excitations of (1.1) a two-parameter continuum of the general form

$$\epsilon(k,q)=I\left\{\left[\sin^2\left[k-\frac{q}{2}\right]+g^2\cos^2\left[k-\frac{q}{2}\right]\right]^{1/2}+\left[\sin^2\left[k+\frac{q}{2}\right]+g^2\cos^2\left[k+\frac{q}{2}\right]\right]^{1/2}\right\}, \quad (2.1)$$

where the two parameters are the wave number q ($0\leq q\leq\pi$) and the variable k ($0\leq k\leq\pi$), which distinguishes different branches in the continuum. $I(\gamma,\Delta)$ and $g(\gamma,\Delta)$ are determined by the anisotropy parameters of the Hamiltonian as described in Ref. 30. For the three sides of the triangle depicted in Fig. 1, I and g are given explicitly by the following expression. (i) For the XY-Heisenberg AFM,

$$I(0,\Delta)=(\pi J\sin\mu)/\mu\ ,\quad g(0,\Delta)\equiv 0\ ,\quad \Delta=\cos\mu\ , \quad (2.2)$$

(ii) for the XY-Ising AFM,

$$I(\gamma,0)=J\ ,\quad g(\gamma,0)=\gamma\ , \tag{2.3}$$

and (iii) for the Heisenberg-Ising AFM,

$$I(\gamma,1-\gamma)=2J\sqrt{\gamma}K(g')/\pi\ ,\quad g'=(1-g^2)^{1/2}\ , \tag{2.4a}$$

and $g(\gamma,1-\gamma)$ is the solution of

$$\pi K(g)/K(g')=\mathrm{sech}^{-1}[(1-\gamma)/(1+\gamma)]\ , \tag{2.4b}$$

where K denotes the complete elliptic integral.

For a typical case this excitation spectrum is sketched in Fig. 2. It consists of two partly overlapping sheets, in the following referred to as $\mathscr{C}_+$ and $\mathscr{C}_-$, respectively. They are bounded by the branches

$$\epsilon_0(q)=I(1+g)\sin q\ , \tag{2.5a}$$

$$\epsilon_1(q)=2I[\sin^2(q/2)+g^2\cos^2(q/2)]^{1/2}\ , \tag{2.5b}$$

$$\epsilon_2(q)=2I[\cos^2(q/2)+g^2\sin^2(q/2)]^{1/2}\ , \tag{2.5c}$$

as indicated in Fig. 2. The special wave number q_c is determined as

$$\cos q_c=(1-g)/(1+g)\ . \tag{2.6}$$

The excitation spectrum has a gap of magnitude $\Delta E=2Ig$. The gap disappears for the XY-Heisenberg line ($\gamma=0$) where g vanishes. In the Ising case ($\Delta=0$, $\gamma=1$) the continuum collapses into a single horizontal branch.

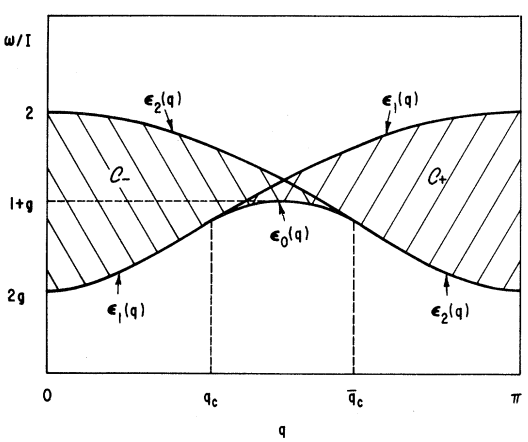

FIG. 2. Excitation spectrum (2.1) of the $S=\frac{1}{2}$ XYZ AFM as predicted in Ref. 30 consists of two partly overlapping sheets $\mathscr{C}_+$ and $\mathscr{C}_-$. Continuum $\mathscr{C}_+$ lies between the boundaries $\epsilon_0(q)$ and $\epsilon_1(q)$ in the range $q_c\le q\le\bar{q}_c\equiv\pi-q_c$ and between $\epsilon_2(q)$ and $\epsilon_1(q)$ for $\bar{q}_c\le q\le\pi$. Continuum $\mathscr{C}_-$ is bounded by $\epsilon_1(q)$ and $\epsilon_2(q)$ for $0\le q\le q_c$ and by $\epsilon_0(q)$ and $\epsilon_2(q)$ for $q_c\le q\le\bar{q}_c$.

It is interesting to know how the excitations (2.1) found via the mapping on a solvable 2D model[30] are distinguished if identified in the following different (but still rigorous) approaches:

(i) For the XY-Heisenberg line the continuum of excitations (2.1) have been identified one by one in the framework of Bethe's formalism as belonging to the class C of "extended" spin-wave states as opposed to "bound" states.[2,31] Therefore, we call (2.1) spin-wave continuum (SWC) excitations.

(ii) For the XY-Ising line the states (2.1) are identified as particle-hole excitations of a free-fermion system with single-particle energies[14]

$$\epsilon_F(k)=I\,\mathrm{sgn}(\cos k)(\cos^2 k+g^2\sin^2 k)^{1/2}\ .$$

The relevance of these excitations for the $T=0$ dynamics is, in general, not known. Let us call a set of excitations relevant for the dynamics if it contributes significantly to the dynamic structure factor,

$$S_{\mu\mu}(q,\omega)=\sum_R e^{-iqR}\int_{-\infty}^{\infty}dt\,e^{i\omega t}\langle S_l^\mu(t)S_{l+R}^\mu\rangle\ . \tag{2.7}$$

At $T=0$, $S_{\mu\mu}$ can be written as

$$S_{\mu\mu}(q,\omega)=d^{-1}\sum_\lambda M_\lambda^\mu\delta(\omega+E_G-E_\lambda)\ ,$$
$$M_\lambda^\mu=\sum_{i=1}^{d}2\pi\,|\langle G_i\,|\,S^\mu(q)\,|\,\lambda\rangle|^2\ , \tag{2.8}$$

where

$$S^\mu(q)=N^{-1/2}\sum_l\exp(iql)S_l^\mu\ ,$$

$|G_i\rangle$, $i=1,\ldots,d$ is the d-fold degenerate ground state with energy E_G, and λ runs over all eigenstates $|\lambda\rangle$ of (1.1) with energies E_λ.

Hence the excitations which are relevant for the $T=0$ dynamics are those which have non-negligible spectral weight M_λ^μ. In Sec. III we shall attempt to answer the question whether the SWC excitations (2.1) belong to or even exhaust the class of relevant states. We can write the SWC contribution to $S_{\mu\mu}(q,\omega)$ more explicitly in the form

$$S_{\mu\mu}(q,\omega)=S_{\mu\mu}^+(q,\omega)+S_{\mu\mu}^-(q,\omega)\ ,$$
$$S_{\mu\mu}^\pm(q,\omega)=M_{\mu\mu}^\pm(q,\omega)D^\pm(q,\omega) \tag{2.9}$$

where the functions $M_{\mu\mu}^\pm(q,\omega)$ represent the matrix elements $|\langle G_j\,|\,S^\mu(q)\,|\,\mathrm{SWC}\rangle|^2$ for excitations in the continuum $\mathscr{C}^\pm$, respectively. $D^\pm(q,\omega)$ are the normalized densities of states in the continua $\mathscr{C}^\pm$, determined by

$$D(q,\omega)=D^{+}(q,\omega)+D^{-}(q,\omega)$$
$$=\frac{1}{2}\int_0^{\pi}dk\delta[\omega-\epsilon(k,q)] \ . \tag{2.10}$$

The explicit evaluation of (2.10) with (2.1) is derived in Sec. III A below.[32]

For a typical example $D^{+}(q,\omega)$ is shown in Fig. 3. It exhibits the characteristic 1D Van Hove singularities at both the upper and lower continuum bounds. These are likely to have their effect on the dynamic structure factor itself as we shall see.

III. MATRIX ELEMENTS AND SPECTRAL WEIGHT DISTRIBUTION

Numerically exact finite-chain calculations[33] have proved to be very useful for the identification of those sets of excitations which play an important role in the $T=0$ dynamics of Hamiltonian (1.1). Several authors have used this method to analyze the spectral weight of the various excitations contributing to $S_{\mu\mu}(q,\omega)$ at $T=0$.[2,3,9,34–36] The results of such investigations have indicated very strongly that most of the spectral weight in $S_{\mu\mu}(q,\omega)$ at $T=0$ is due to the SWC excitations (2.1). Exact results prove that for $\Delta=0$ the SWC excitations even exhaust all spectral weight in $S_{zz}(q,\omega)$ at $T=0$.[37]

Given the strong evidence that the SWC excitations are predominant in the $T=0$ dynamics structure factor $S_{\mu\mu}(q,\omega)$ of Hamiltonian (1.1) at $T=0$, it is legitimate to study the SWC contributions to $S_{\mu\mu}(q,\omega)$ solely, assuming that a good approximation for these contributions represents a good approximation for the dynamic structure factor itself. Having conjectured the form (2.9) for the SWC contributions to $S_{\mu\mu}(q,\omega)$, and having evaluated an exact result for their density of states $D^{\pm}(q,\omega)$, we are left with the task of providing results for the matrix element functions $M^{\pm}_{\mu\mu}(q,\omega)$ in order to determine $S_{\mu\mu}(q,\omega)$. In the following, we present the exact solution for $S_{zz}(q,\omega)$ of the XY-Ising AFM (Sec. III A); we review the result of $S_{zz}(q,\omega)$ for the XY-Heisenberg AFM from a calculation based on sum rules (Sec. III B), and we propose two approaches to calculate $S_{zz}(q,\omega)$ of the Heisenberg-Ising AFM (Sec. III C).

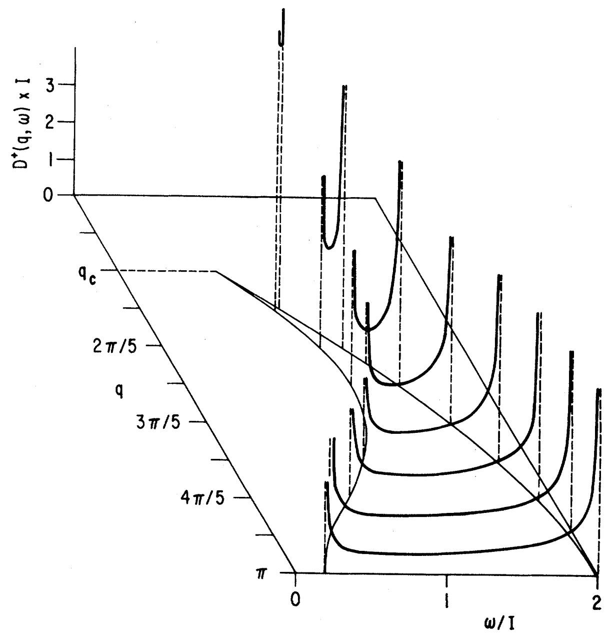

FIG. 3. Normalized density of states $D^{+}(q,\omega)$ of the SWC excitations (2.1) as a function of frequency for wave numbers $q=n\pi/10$, $n=0,1,\ldots,10$, and $g=0.1$. $D^{-}(q,\omega)$ is simply imagined from this figure by noting the relation $D^{-}(q,\omega)=D^{+}(\pi-q,\omega)$.

A. XY-Ising AFM ($0\leq\gamma\leq 1$, $\Delta=0$)

Here we derive a closed form analytic expression for the exact $S_{zz}(q,\omega)$ of the $S=\frac{1}{2}$ XY-Ising AFM at $T=0$. In the fermion representation of spin operators the time-dependent correlation function $\langle S_l^z(t)S_{l+R}^z\rangle$ can be expressed as a density correlation function of a system of noninteracting fermions. An integral expression for this quantity has been given in Ref. 14 (see also Ref. 17). An integral expression for the dynamic structure factor is readily obtained by Fourier transform.[18] For $T=0$ it reads

$$S_{zz}(q,\omega)=\frac{1}{2}\int_0^{\pi}dk[1-f(k,q)]\delta[\omega-\epsilon(k,q)] \ , \tag{3.1a}$$

$$f(k,q)=\frac{\sin\left[k-\frac{q}{2}\right]\sin\left[k+\frac{q}{2}\right]-g^2\cos\left[k-\frac{q}{2}\right]\cos\left[k+\frac{q}{2}\right]}{\left[\sin^2\left[k-\frac{q}{2}\right]+g^2\cos^2\left[k-\frac{q}{2}\right]\right]^{1/2}\left[\sin^2\left[k+\frac{q}{2}\right]+g^2\cos^2\left[k+\frac{q}{2}\right]\right]^{1/2}} \ , \tag{3.1b}$$

where $\epsilon(k,q)$ is given by (2.1) and $I=J$, $g=\gamma$ according to (2.3). Evidently, the SWC excitations (2.1) exhaust all the spectral weight of $S_{zz}(q,\omega)$. Hence representation (2.9) is exact.

The evaluation of the integral (3.1a) requires the knowledge of the roots of the δ-function argument. We find that for $(q,\omega)\in\mathscr{C}_+$ there are two roots k_+ and $\pi-k_+$, and for $(q,\omega)\in\mathscr{C}_-$ there are two other roots,

k_- and $\pi - k_-$, determined by

$$\cos 2k_{\pm} = \frac{\omega^2 \cos q \pm T(q,\omega)}{(1-g^2)\sin^2 q} , \tag{3.2a}$$

$$T(q,\omega) = [\omega^2 - I^2(1-g)^2 \sin^2 q]^{1/2} [\omega^2 - I^2(1+g)^2 \sin^2 q]^{1/2} . \tag{3.2b}$$

Thus (3.1) can be written in the form (2.9) with

$$S_{zz}^{\pm}(q,\omega) = |\epsilon'(k_{\pm},q)|^{-1}[1-f(k_{\pm},q)] , \quad (q,\omega) \in \mathscr{C}_{\pm} \tag{3.3}$$

where $\epsilon'(k,q) = (\partial/\partial k)\epsilon(k,q)$. The two factors in (3.3) are identified as the density of SWC states $D^{\pm}(q,\omega)$ and their matrix elements $M_{zz}^{\pm}(q,\omega)$, respectively. The explicit expressions read

$$D^{\pm}(q,\omega) = |\epsilon'(k_{\pm},q)|^{-1} = n_{\pm}(q,\omega)/e_{\pm}(q,\omega) , \tag{3.4a}$$

$$M_{zz}^{\pm}(q,\omega) = [1-f(k_{\pm},q)] = z_{\pm}(q,\omega)/n_{\pm}(q,\omega) , \tag{3.4b}$$

$$S_{zz}^{\pm}(q,\omega) = D^{\pm}(q,\omega) M_{zz}^{\pm}(q,\omega) = z_{\pm}(q,\omega)/e_{\pm}(q,\omega) , \tag{3.4c}$$

where

$$n_{\pm}(q,\omega) = (2\sin^2 q)^{-1}\{[\omega^2 - I^2(1+g^2)\sin^2 q] \pm \cos q T(q,\omega)\} , \tag{3.5a}$$

$$e_{\pm}(q,\omega) = (2\sin^2 q)^{-1} T(q,\omega)[2I^2(1+g^2)\sin^2 q - \omega^2(1+\cos^2 q) \mp 2\cos q T(q,\omega)]^{1/2} , \tag{3.5b}$$

$$z_{\pm}(q,\omega) = \left[4(1-g^2)\sin^2\frac{q}{2}\right]^{-1} [\omega^2 - I^2(1-g^2)\sin^2 q \pm T(q,\omega)] - \gamma^2 \left[4(1-g^2)\cos^2\frac{q}{2}\right]^{-1} [\omega^2 + I^2(1-g^2)\sin^2 q \mp T(q,\omega)] , \tag{3.5c}$$

for any (q,ω) confined to the continua $\mathscr{C}_+$ and $\mathscr{C}_-$, respectively. The expression for $S_{zz}(q,\omega)$ simplifies considerably for $q=0$ and $q=\pi$,

$$S_{zz}(0,\omega) = S_{zz}^{-}(0,\omega) = \frac{2g^2(4I^2-\omega^2)^{1/2}}{(1-g^2)\omega(\omega^2-4g^2I^2)^{1/2}} , \tag{3.6a}$$

$$S_{zz}(\pi,\omega) = S_{zz}^{+}(\pi,\omega) = \frac{2(\omega^2-4g^2I^2)^{1/2}}{(1-g^2)\omega(4I^2-\omega^2)^{1/2}} . \tag{3.6b}$$

For $g=\gamma=0.1$, corresponding to a small anisotropy, the functions $D^{\pm}(q,\omega)$, $M_{zz}^{\pm}(q,\omega)$, and $S_{zz}^{\pm}(q,\omega)$ are shown in Figs. 3–5, respectively.[38] The matrix-element function $M_{zz}^{+}(q,\omega)$ is seen to have an almost flat shape except near the lower boundary. Consequently, $S_{zz}^{+}(q,\omega)$ is dominated by density-of-states effects. This is reflected by the divergences in $S_{zz}^{+}(q,\omega)$ along the boundaries $\epsilon_1(q)$ and $\epsilon_0(q)$ of $\mathscr{C}_+$. However, it is interesting to note that the zero in $M_{zz}^{+}(q,\omega)$ at $\omega=\epsilon_2(q)$, $\bar{q}_c \le q \le \pi$, overcomes the divergence in $D^{+}(q,\omega)$ at the same frequency, causing $S_{zz}^{+}(q,\omega)$ to drop to zero. The function $M_{zz}^{-}(q,\omega)$ is very small everywhere in $\mathscr{C}_-$ except close to the lower bound, and goes to zero at $\omega=\epsilon_2(q)$. As a result, the spectral weight of $S_{zz}^{-}(q,\omega)$ is strongly peaked at the lower bound of $\mathscr{C}_-$, again reflecting the divergence of the density of states. For $q_c \le q \le \bar{q}_c$, the dynamic structure factor has two peaks.

B. *XY*-Heisenberg AFM ($\gamma=0$, $0\le\Delta\le 1$)

In order to have a second "anchor point" for the study of the more complicated *XYZ* AFM we review briefly the principal results of previous work on the planar AFM.[3,4] The exact result for $S_{zz}(q,\omega)$ at $T=0$ is known only for $\Delta=0$, given by (3.3)–(3.5) in the limit $\gamma\to 0$,

$$D^{+}(q,\omega) = [\epsilon_1^2(q)-\omega^2]^{1/2} , \quad M_{zz}^{+}(q,\omega) = 2 \quad \text{for } \epsilon_0(q) \le \omega \le \epsilon_1(q) , \tag{3.7a}$$

$$D^{-}(q,\omega) = [\epsilon_2^2(q)-\omega^2]^{-1/2} , \quad M_{zz}^{-}(q,\omega) = 0 \quad \text{for } \epsilon_0(q) \le \omega \le \epsilon_2(q) , \tag{3.7b}$$

with

$$\epsilon_0(q) = I\sin q , \quad \epsilon_1(1) = 2I\sin(q/2) , \quad \epsilon_2(q) = 2I\cos(q/2) . \tag{3.7c}$$

Only continuum $\mathscr{C}_+$ (now gapless) contributes to $S_{zz}(q,\omega)$,

$$S_{zz}(q,\omega) = 2[\epsilon_2^2(q)-\omega^2]^{-1/2} , \quad \epsilon_0(q) \le \omega \le \epsilon_1(q) , \quad \Delta=0 . \tag{3.8}$$

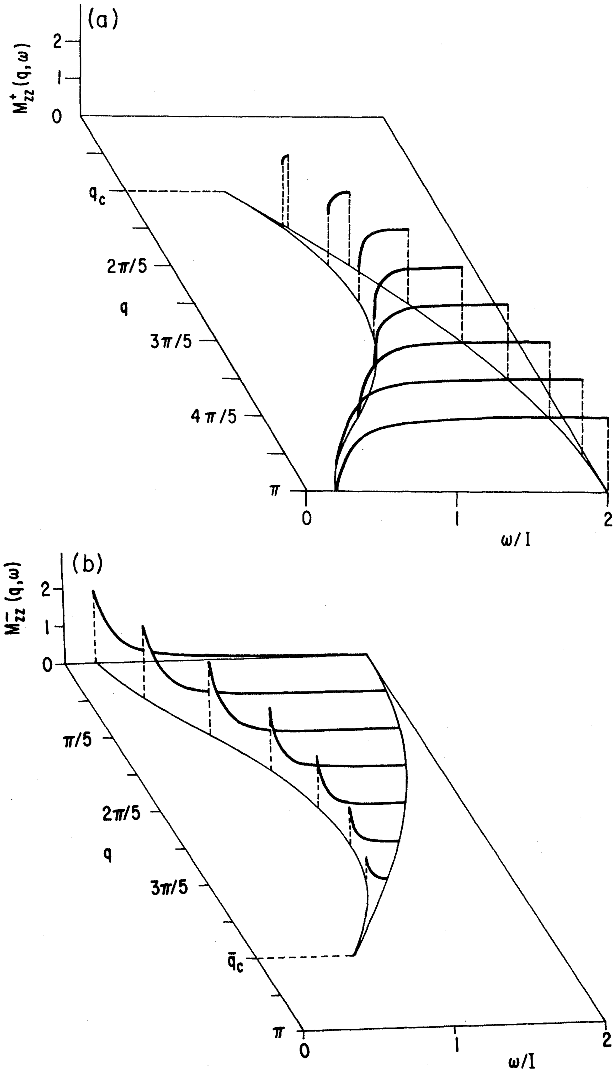

FIG. 4. Normalized squared matrix elements $M^+_{zz}(q,\omega)$ and $M^-_{zz}(q,\omega)$ of the SWC excitations (2.1) for the *XY*-Ising AFM as a function of frequency for wave numbers of $q=n\pi/10$, $n=0,1,\ldots,10$, and $g=\gamma=0.1$.

For $0<\Delta\leq 1$, finite-chain results have indicated very strongly that almost all the spectral weight in $S_{zz}(q,\omega)$ at $T=0$ is still due to $\mathscr{C}_+$ states, but the matrix elements $M^+_{zz}(q,\omega)$ are no longer constant.[2,3,35] In Ref. 4, an analytic expression for $M^+_{zz}(q,\omega)$ has been proposed on the basis of sum-rule arguments

$$M^+_{zz}(q,\omega)\propto\left[\frac{\epsilon_1^2(q)-\omega^2}{\omega^2-\epsilon_0^2(q)}\right]^\alpha ,$$

$$\alpha=\frac{\pi/2-\cos^{-1}\Delta}{\pi-\cos^{-1}\Delta} . \quad (3.9)$$

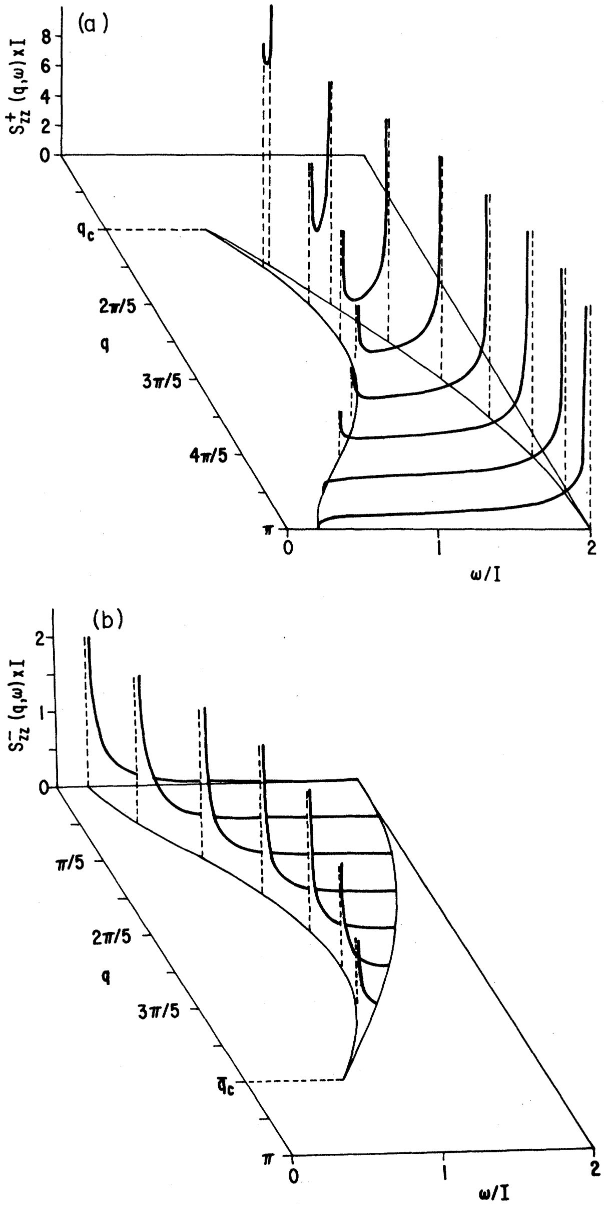

FIG. 5. Dynamic structure factors $S^+_{zz}(q,\omega)$ and $S^-_{zz}(q,\omega)$ of the SWC excitations (2.1) for the *XY*-Ising AFM as a function of frequency for wave numbers $q=n\pi/10$, $n=0,1,\ldots,10$, and $g=\gamma=0.1$.

In combination with the exact density of states $D^+(q,\omega)$ of (3.7a) this leads to the result

$$S_{zz}(q,\omega)=A_+[\omega^2-\epsilon_0^2(q)]^{-\alpha}\times[\epsilon_1^2(q)-\omega^2]^{\alpha-1/2} , \quad \epsilon_0(q)\leq\omega\leq\epsilon_1(q) . \quad (3.10)$$

The Δ-dependent prefactor A_+ was determined in Ref. 3. For $\Delta=0$ we get $\alpha=0$, $A_+=2$, recovering the exact result (3.8). For $0<\Delta<1$, $S_{zz}(q,\omega)$ has a two-peak structure[39] as a function of ω. The main feature is that as Δ grows from zero, an increasing amount of spectral weight is transferred from a region close to the upper continuum boundary to a region close to the lower continuum boundary. This behavior is nicely reproduced for $\Delta \ll 1$ by a perturbation calculation in the fermion representation.[5]

C. Heisenberg-Ising AFM ($0 \leq \gamma \leq 1$, $\Delta = 1-\gamma$)

The exact result[3,4] for $S_{zz}(q,\omega)$ of the XY-Ising AFM and the result (3.10) for $S_{zz}(q,\omega)$ of the XY-Heisenberg AFM provide a sound basis for calculations aiming towards a reliable prediction for $S_{zz}(q,\omega)$ of the Heisenberg-Ising AFM. This would be most desirable for an interpretation of the observed line shapes of neutron scattering experiments on $CsCoCl_3$.

Both the nonperturbative approach[4] and the perturbation calculation[5] pursued for the XY-Heisenberg line ($\gamma=0$) of Fig. 1 can, in principle, be generalized to any parallel line at $\gamma \neq 0$. An advantage of the perturbation approach in the fermion representation over the approach used in Ref. 9 is that already the result of the unperturbed Hamiltonian exhibits nontrivial dynamical properties and has many features in common with experimental data on $CsCoCl_3$. In fact, for small q, $S_{zz}(q,\omega)$ of $H(\gamma,0)$ has the form of a sharp asymmetric peak at the lower continuum boundary [see Fig. 5(b)], very much in agreement with the experimental findings (see Fig. 9 of Ref. 11). For larger q, a second peak at higher frequency appears in $S_{zz}(q,\omega)$ of the XY-Ising AFM [see Fig. 5(a)]. Preliminary perturbation results[19] suggest that the effect of the fermion interaction is to shift the spectral weight in $S_{zz}^{+}(q,\omega)$ towards the lower continuum boundary. Nevertheless, the peak in $S_{zz}^{+}(q,\omega)$ at the upper boundary of $\mathscr{C}_+$ seems to persist in the presence of a weak interaction. It is interesting to note that the experimental data presented in Refs. 11 and 12 also indicate the existence of weak resonances at higher frequencies. Progress in both approaches suggested will be reported on in a subsequent publication.

ACKNOWLEDGMENTS

The authors have benefited from interesting and stimulating discussions with Professor J. C. Bonner. This work was supported by the Swiss National Science Foundation and by the U. S. National Science Foundation under Grant No. DMR80-10819.

*Present address: Institute for Theoretical Physics, State University of New York, Stony Brook, N. Y. 11794

[1]J. C. Bonner, J. Appl. Phys. 49, 1299 (1978); H. J. Mikeska, *ibid.* 52, 1950 (1981); H. Beck, M. W. Puga, and G. Müller, *ibid.* 52, 1998 (1981). References to the earlier literature are found in these recent review articles.

[2]G. Müller, H. Thomas, H. Beck, and J. C. Bonner, Phys. Rev. B 24, 1429 (1981).

[3]G. Müller, H. Thomas, M. W. Puga, and H. Beck, J. Phys. C 14, 3399 (1981).

[4]G. Müller, Phys. Rev. B 26, 1311 (1982).

[5]H. Beck and G. Müller, Solid State Commun. 43, 399 (1982).

[6]Y. Endoh, G. Shirane, R. J. Birgeneau, P. M. Richards, and S. L. Holt, Phys. Rev. Lett. 32, 170 (1974).

[7]I. U. Heilmann, G. Shirane, Y. Endoh, R. J. Birgeneau, and S. L. Holt, Phys. Rev. B 18, 3530 (1978).

[8]Dynamical experimental results on the quasi-1D planar $S=\frac{1}{2}$ AFM Cs_2CoCl_4 are eagerly awaited.

[9]N. Ishimura and H. Shiba, Prog. Theor. Phys. 63, 743 (1980).

[10]J. D. Johnson and B. M. McCoy, Phys. Rev. A 6, 1613 (1972).

[11]H. Yoshizawa, K. Hirakawa, S. K. Satija, and G. Shirane, Phys. Rev. B 23, 2298 (1981).

[12]S. E. Nagler, W. J. L. Buyers, and R. L. Armstrong, J. Appl. Phys. 52, 1971 (1981).

[13]Note the different parametrization of the Heisenberg-Ising Hamiltonian

$$H=2J'\sum[S_l^zS_{l+1}^z+\epsilon(S_l^xS_{l+1}^x+S_l^yS_{l+1}^y)]\ , \quad 0\leq\epsilon\leq 1\ ,$$

used in Refs. 9, 11, and 12 as compared to our $H(\gamma,1-\gamma)$. The relations are $J'=\frac{1}{2}J(1+\gamma)$, $\epsilon=(1-\gamma)/(1+\gamma)$. The easy axis is z in H' and x in H. $S_{xx}(q,\omega)$ of Refs. 9, 11, and 12 corresponds to our $S_{zz}(q,\omega)$ and vice versa.

[14]T. Niemeijer, Physica 36, 377 (1967).

[15]S. Katsura, T. Horiguchi, and M. Suzuki, Physica 46, 67 (1970).

[16]B. M. McCoy, E. Barouch, and D. B. Abraham, Phys. Rev. A 4, 2331 (1971).

[17]J. H. H. Perk, H. W. Capel, and T. J. Siskens, Physica 89A, 304 (1977).

[18]M. W. Puga and H. Beck, J. Phys. C 15, 2441 (1982).

[19]G. Müller (unpublished).

[20]H. Bethe, Z. Phys. 71, 205 (1931).

[21]J. des Cloizeaux and J. J. Pearson, Phys. Rev. 128, 2131 (1962).

[22]Y. Yamada, Prog. Theor. Phys. 41, 880 (1969).

[23]R. Orbach, Phys. Rev. 112, 309 (1958).

[24]J. des Cloizeaux and M. Gaudin, J. Math. Phys. 7, 1384 (1966). An erroneous conclusion in this reference has been corrected by M. Fowler, Phys. Rev. B 17, 2989 (1978); J. Phys. C 11, L977 (1978).

[25]N. Ishimura and H. Shiba, Prog. Theor. Phys. 57, 1862 (1977).

[26]E. H. Lieb, T. D. Schultz, and D. C. Mattis, Ann. Phys.

(N.Y.) 16, 407 (1961).

[27]S. Katsura, Phys. Rev. 127, 1508 (1962).

[28]B. Sutherland, J. Math. Phys. 11, 3183 (1970).

[29]R. J. Baxter, Ann. Phys. (N.Y.) 70, 323 (1972).

[30]J. D. Johnson, S. Krinsky, and B. M. McCoy, Phys. Rev. A 8, 2526 (1973).

[31]R. B. Griffiths, Phys. Rev. 133, A768 (1964).

[32]See Eqs. (3.3)—(3.5) for the explicit result.

[33]Such calculations consist in the numerical diagonalization of H for finite N (with N as large as the computer facilities allow), and in the evaluation of the squared matrix elements M_{λ}^{μ} of Eq. (2.8) using the exact eigenfunctions.

[34]G. Müller and H. Beck, J. Phys. C 11, 483 (1978).

[35]G. Müller, H. Beck, and J. C. Bonner, Phys. Rev. Lett. 43, 75 (1979).

[36]T. Schneider and E. Stoll, Phys. Rev. Lett. 47, 377 (1981); J. Appl. Phys. 53, 1850 (1982).

[37]Note, however, that there is evidence from sum-rule arguments [P. C. Hohenberg and W. F. Brinkman, Phys. Rev. B 10, 128 (1974)], from finite-chain extrapolations (Ref. 34), and from rigorous calculations (Ref. 16) that some spectral weight in $S_{zz}(q,\omega)$ at $\Delta\neq0$ and in $S_{xx}(q,\omega)$ at arbitrary Δ must be due to higher-lying excitations.

[38]See also Figs. 6 and 7 of Ref. 18.

[39]The line shapes of the result (3.9) have been discussed in Ref. 3 (Fig. 4) and in Ref. 4 (Fig. 1).